Key Engineering Materials Vols. 525-526 (2013) pp 485-488

doi:10.4028/www.scientific.net/KEM.525-526.485

Relation between structural size and the discretization density of brittle homogeneous lattice models

Miroslav Vořechovský[1, a], Jan Eliáš[1,b]

[1]Institute of Structural Mechanics, Faculty of Civil Engineering, Brno University of Technology, Brno, Czech Republic

[a] vorechovsky.m@fce.vutbr.cz, [b] elias.j@fce.vutbr.cz

Keywords: lattice model, brittle elements, mesh size, bent beams, size effect

Abstract. This paper contains the results of an investigation into the effect of the discretization of lattice models. The study is performed with homogeneous models where all elements share the same strength. Elemental constitutive law is linearly-brittle, meaning that elements behave linearly but are completely removed from the structure as soon as they reach the limit of their strength. The relation between structural size and discretization density is studied with unnotched beams loaded in three point bending (modulus of rupture test). We report the results for regular discretization and irregular networks obtained via Voronoi tessellation. This is carried out for two types of models: these being with and without rotational springs (normal and shear springs are always present). The numerically obtained dependence of strength on discretization density is compared to the analytical size effect formula.

Introduction and brief model description

The lattice representation of material is a well-established approach to modeling the failure of brittle and quasibrittle materials. Material is treated as a set of discrete rigid-like elements inter-connected by springs. In the classical version of these models, the connections behave in an elasto-brittle manner until some failure criteria are reached [1-3]. Then, the elements are completely removed from the structure. The response of these brittle models appears to be highly dependent on discretization density [4]; this dependence can be avoided by the application of material mesostructure [5].

In this contribution we focus only on homogeneous brittle lattice models (i.e. without mesostructure). Thus, all lattice connections share the same elastic parameters and strength criterion. We assume that varying the network density in homogeneous models corresponds to changes in the structural size of the structure modeled. These mesh-density effects are studied for specimens that fail due to a crack initiated from a smooth surface. In particular, we have performed numerous simulations with unnotched three-point-bent specimens. The span $S = 3D$, where D is the specimen depth.

The model used is a rigid-body-spring network in accordance with a paper by Bolander & Saito [6]. The fracture criteria are taken from the same article, i.e. a Mohr-Coulomb surface with tension cut-off is adopted. The solution proceeds in linear elastic steps that are scaled so that one connection breaks at each step [7]. The irregular network is generated by Voronoi tessellation on a set of pseudo-randomly placed nuclei with limited maximal mutual distance $l_{\min}$. By changing $l_{\min}$ one can control the mesh density. The IRN model (with an irregular network) is compared to a network with locally regular geometry (REN). In the REN model, the crack can only propagate along the axis of symmetry through regularly placed squared elements of *exact* $l^{\min}$ size. The rest of the specimen is meshed by a lattice of irregular geometry. Consequently, the obtained nominal forces are scattered.

Two different versions of the mechanical model are studied. They differ in how internal forces (between rigid bodies) are transmitted through the connections of adjacent facets. In the first model type (denoted NS), only normal and shear springs act. In the NSR model type, rotational springs transferring local bending moments are also added. However, only stresses in normal and shear springs contribute to the fracture criteria in both model types.

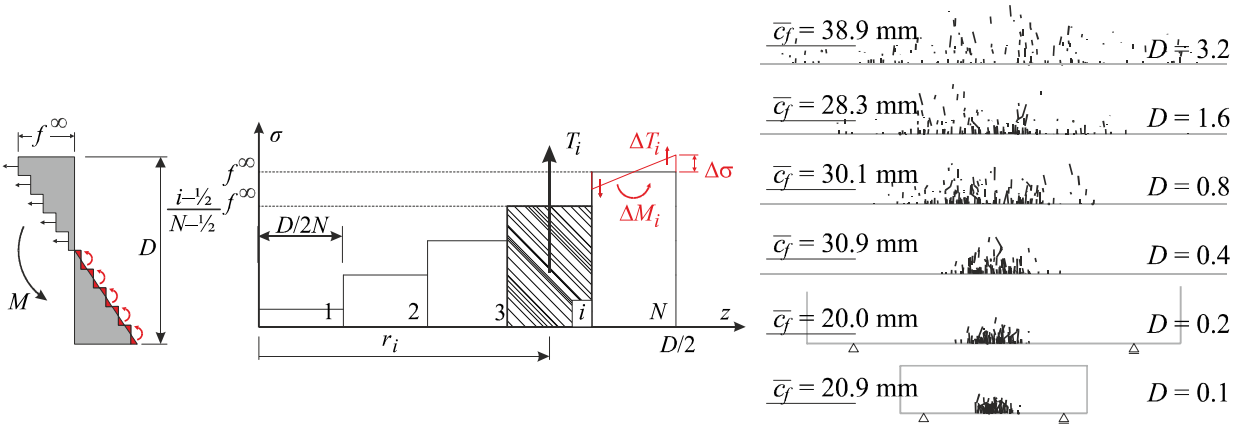

Figure 1: Left: On derivation of the peak moment in a bent specimen. Right: Crack patterns at the peak load for various sizes of the IRN beam. The left horizontal lines indicate the average height c_f.

Size effect simulations and formulas

The size of a concrete specimen typically affects the observed nominal strength. Several sources of this phenomenon have been documented [8]; the statistical and deterministic size effects are the two most significant. Since there is no internal length in our constitutive law/model we can represent varying size by varying network density. The characteristic size (depth) D is kept constant at a reference size D_0 = 0.1 m, whereas the network density $l^{\min}$ is varied; we can mimic the varying of the intrinsic size D by writing $D = D_0 \cdot l_0^{\min} / l^{\min}$, where $l_0^{\min}$ is the selected reference mesh density.

Since we are dealing, in fact, with models of the same size, it is not necessary to report the size dependence on nominal strength (nominal stress at peak load). It suffices to report the loading forces $F(D)$. On the other hand, however, the lengths (e.g. the crack length) must be recalculated.

Let us now deliver a closed-form expression for the observed size effect. Consider the midspan rectangular cross-section BD. The depth is discretized into $2N$ rigid bodies' contacts of the same size, and therefore the stress profile is a piecewise constant function along the depth D and approximates the actual linear profile. When the outermost spring reaches the extreme tensile stress f^∞, the cross-section reaches its maximum bending moment M. Due to the symmetry along the neutral axis we can only consider the lower half of the depth (N elements) and calculate the bending moment as a doubled sum of force contributions multiplied by the corresponding arms. Each i-th force contribution can be written as (Figure 1 left): $T_i = (i-1/2)BDf^\infty / 2N(N-1/2)$. Each such force has the following arm from the neutral axis: $r_i = D(i-1/2)/2N$. The resisting moment is double the sum for moment contributions:

$$M(N) = 2\sum_{i=1}^{N} T_i r_i = \frac{BD^2}{4N^2}\frac{f^\infty}{N-1/2}\sum_{i=1}^{N}\left(i-\frac{1}{2}\right)^2 = \frac{BD^2}{6}f^\infty\left(\frac{2N+1}{2N}\right) \tag{1}$$

As N tends to infinity, the bending moment converges to the well-known value $M^\infty = f^\infty BD^2/6$. The external bending moment equals $M = F/2 \cdot 3D/3$. Equalizing these two expressions and considering that $l^{\min}=D/(2N)$, one ascertains that:

$$F = \frac{2BD}{9}f^\infty\left(\frac{2N+1}{2N}\right) = \underbrace{\overbrace{\left(\frac{2BD}{9}\right)}^{c} f^\infty}_{F^\infty}\left(1+\frac{l_0^{\min}}{D}\right) = F^\infty\left(1+\frac{l_0^{\min}}{D}\right) = F^\infty\left(1+\frac{D_b}{D}\right) \tag{2}$$

We can introduce a new length constant, $D_b = l_0^{\min}$. Then, Eq. (2) becomes identical with Bažant's size effect formula for type 1 deterministic size effect (see pages 41–43 of [8]). The increment to the asymptotic force F^∞ is inversely proportional to D and therefore diminishes for large D (or small $l^{\min}$). What remains to be clarified is the choice of the extreme stress f^∞. An obvious

choice would be the direct tensile strength (f_l^∞= 5 MPa) of the model. This is because very large specimens fail at the initiation of a crack right at the midspan bottom face, which must therefore equal the tensile strength, yielding the asymptotic force F_l^∞ = 11.11 kN. Unfortunately, the stress profile in not perfectly linear in reality. The real stress profile is affected by wall-like stress distribution (the span of the beam is only 3*D*) and by the local compressive stress concentration around the point load. The nonzero Poisson's ratio causes additional deviation from the linear stress profile; see [9] or [10]. As an approximation, we used a nonlinear least-square fitting procedure to determine the two free parameters D_b and F^∞ in Eq. 2. The fits are plotted in Figure 2 and compared to the computed data.

Now, what if the rotational springs are employed? In each element (or contact area), its spring adds a new additional moment ΔM_i; see the last strip in Figure 1 left. These contributions are equal. In each bin there is a pair of forces ΔT_i that represent two triangles (below and above the constant stress σ_i. Each of these triangles are as long as half of the strip (=*D*/(4*N*)) and the maximum stress difference is $\Delta\sigma$. The stress $\Delta\sigma$ is one half of the difference between the current strip and the adjacent strip: $\Delta\sigma = \left(\sigma_i - \sigma_{i-1}\right)/2 = f^\infty/(2N-1)$. The pair of forces ΔT_i representing the two triangles are:

$$\Delta T_i = \frac{1}{2}\Delta\sigma \cdot B \cdot \frac{D}{4N} = \Delta\sigma \frac{BD}{8N} = \frac{f^\infty}{2N-1} \cdot \frac{BD}{8N} \tag{3}$$

Each of these two forces act over the distance of *D*/(6*N*) from the "neutral" state and form an additional increase in the total bending moment. The magnitude of each such moment contribution (in each strip-bin) is twice the arm multiplied by the force ΔT_i: $\Delta M_i = 2 \cdot \Delta T_i \cdot D/6N$. In total, there are 2*N* such partial moments over the whole cross-section and therefore the total moment increment is 2*N* × the contribution ΔM_i and $\Delta M = 2N \cdot \Delta M_i = f_\infty BD^2/12N\left(2N-1\right)$. The moment increment is not reflected in the failure condition. Transforming it into the increment of maximal force gives:

$$\Delta F = \frac{4}{3D}\Delta M = F^\infty \frac{1}{2N\left(2N-1\right)} = F^\infty \frac{l_0^{\min}}{D}\frac{l_0^{\min}}{D-l_0^{\min}} \tag{4}$$

Adding this increment to the total force from Eq. 2 yields the upgraded size dependence. The increment ΔF increases the maximal load especially for small sizes because it is proportional to the inverse of D^2 while the increment to the asymptotic stress in Equations 2 was only inversely proportional to *D*. The irregularity of the network geometry (IRN) allows the model to choose the "weakest" area to initiate and propagate the crack. Contrary to REN, where the rupture of the first connection leads to the failure of the whole beam, the load applied to break the first spring in the IRN model (elastic limit in Fig. 2) is, on average, much lower than the peak forces. The peak forces in IRN models are greater than those of REN models, whereas the elastic limits are lower in IRN models.

Qualitatively, however, both force dependencies of IRN are similar to REN and follow the tendency proposed by Eq. 2 and Eq. 4, respectively. The deviations for larger specimens (finer mesh densities) are caused by the local stress deviation described earlier, meaning namely the stress fluctuations in the lowermost layer caused by Poisson's ratio.

Instead of one crack, many small cracks are created inside the bottom area of the IRN specimen (Figure 1b) and the model allows for the redistribution of forces after many such local ruptures. These cracks do not form a continuous line at maximal load. The fact that the zone has, on average, approximately the same height for all sizes (over size ratio 1:32) supports our claim that the data can be approximated reasonably well by Bažant's size effect formula, which is similar to Eq. 2.

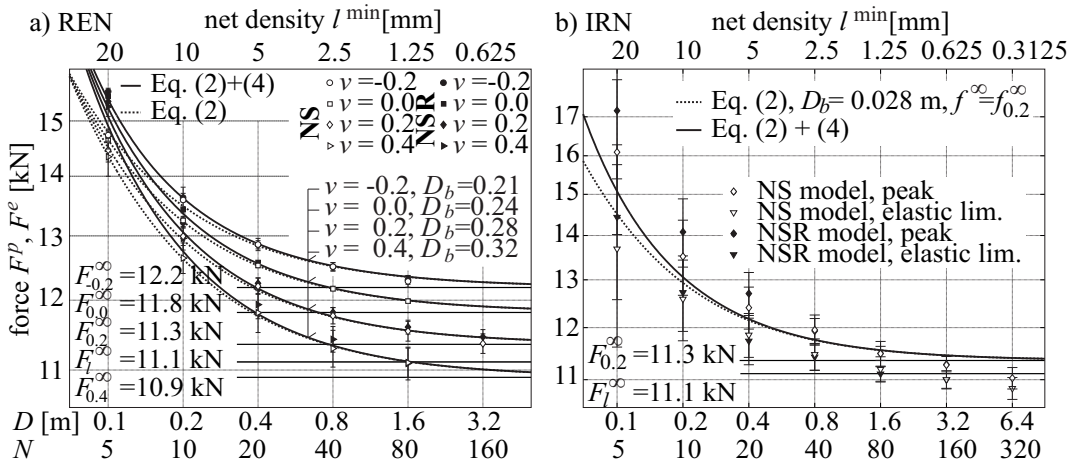

Figure 4: Dependency of the peak load on the network density (or structural size D) and comparison to the size effect formulas (Equations 2 and 4). a) REN meshes with a different Poisson's ratio. b) Plot of elastic limits and peak loads of beams with an irregular network. Average values and standard deviations are computed from 50 realizations for every size.

Summary

The effect of the discretization of homogeneous lattice models was studied on three-point bending simulations. We report the results for regular and irregular geometry. The dependence of strength is compared to derived size effect formulas and we show that the fineness of the discretization of specimens of the same size can mimic variations in the size of lattice models with the same discretization.

Acknowledgement. This research was conducted with the financial support of the Czech Science Foundation, projects GACR P105/10/J028 and GD103/09/H08.

References

[1] G. Lilliu, J.G.M. van Mier: Eng. Fract. Mech. Vol. 70 (2003), p. 927–941.

[2] J.E. Bolander, H. Hikosaka, W.-J. He: Eng. Computation. Vol. 15 (1998), p. 1094–1116.

[3] J. Eliáš, H. Stang: Int. J. Fracture, available online, (2012), DOI 10.1007/s10704-012-9677-3

[4] A. Jagota, S. J. Bennison: Model. Simul. Mater. Sc., Vol. 3 (1995), p. 485–501.

[5] J. Eliáš, M. Vořechovský: Key Eng. Mat., Vol. 488-489 (2012), p. 29-32

[6] J.E. Bolander, S. Saito: Eng. Fract. Mech., Vol. 61 (1998), p. 569–591.

[7] J. Eliáš, M. Vořechovský, P. Frantík: Eng. Fract. Mech., Vol. 77 (2010), p. 2263–2276.

[8] Z.P. Bažant: *Scaling of Structural Strength* (Elsevier Butterworth-Heinemann, 2005).

[9] M. Vořechovský, J. Eliáš, in: Computational Modelling of Concrete Structures (EURO-C 2010), edited by Bicanic et al, CRC Press (2010), ISBN 978-0-415-58479-1, p. 419–428.

[10] M. Vořechovský, J. Eliáš, in: Proceedings of the Tenth International Conference on Computational Structures Technology, Civil-Comp Press (2010).